

A FIELD STUDY OF THE MEAN PRESSURE ABOUT A WINDBREAK

JOHN D. WILSON

Department of Earth & Atmospheric Sciences, University of Alberta, Edmonton, Alberta, T6G 2E3, Canada

(Received in final form 12 May, 1997)

Abstract. To provide additional field data for assessing windbreak flow models, mean ground-level pressure has been measured upstream and downstream from a long porous fence (height $H = 1.25$ m, resistance coefficient $k_r = 2.4$). Measurements were made during periods of near-neutral stability and near-normally incident flow, with the fence standing on bare soil (roughness length, $z_0 \approx 0.8$ cm; $H/z_0 \approx 160$), or within a plant canopy. The mean pressure field, measured far from the ends of the fence, was found to be quite insensitive to mean wind direction ($\bar{\alpha}$, zero for perpendicular flow), for $|\bar{\alpha}|$ less than about 25° .

In the absence of a canopy, during each measurement period the minimum pressure occurred at the closest sampling location to leeward of the windbreak, the pressure-gradient in most cases being maximally-adverse in the immediate lee, and decaying with increasing downwind distance (x). On one day of measurements, however, the pressure gradient over $2 \leq x/H \leq 6$ ($H =$ windbreak height) resembled the leeward 'plateau' identified by Wang and Takle in their numerical studies. Perhaps this 'occasional' feature was only due to instrument error. Nevertheless a 'plateau' of sorts was indicated in similar measurements by Judd and Prendergast (with $H = 1.92$ m, $z_0 \approx 1.2$ cm; $H/z_0 \approx 160$, $k_r \approx 3$). Therefore, existence of a leeward pressure plateau behind a thin fence cannot be definitely ruled out.

When the windbreak was placed in a canopy, minimum surface pressure was displaced downwind. This agrees with the wind-tunnel study of Judd, Raupach and Finnigan, and is consistent with a simple simulation reported here.

Key words: Windbreak flow, Shelter, Windbreak flow models, Micrometeorological models

1. Introduction

A long-term goal of research in windbreak aerodynamics is to provide a basis for the design of windbreaks, or windbreak networks, which are often present for the reason of protecting a crop. However it is not certain whether the models* that express our understanding have yet dealt correctly with the simplest case, that of a single windbreak on bare ground. Wilson (1985; hereafter W85) found that, independent of which turbulence closure he adopted, simulated mean velocity fields $\bar{u}(x, z)$ recovered somewhat more slowly far downstream (large x/H) toward the approach profile $\bar{u}_0(z)$, than suggested by the data of Bradley and Mulhearn (1983). However, using what seems a very similar model, Wang and Takle (1995; hereafter WT) reported much better agreement with the same data. From this discrepancy

* Models that may be entirely empirical, as in Schwartz et al. (1995), or based on the Navier-Stokes equations in the form of large eddy simulations (Patton et al., 1996) or solutions to the Reynolds equations (e.g., Hagen et al. 1981, and other work cited below) providing the spatial fields of mean velocity and other statistical properties.

arises the present study, concerning the mean pressure field $\bar{p}(x, z)$ about a porous fence: because according to WT these two similar models differ qualitatively in their prediction of the mean pressure along the ground,* and WT (p. 167) considered that difference to explain their faster windspeed recovery. In particular Wilson's simulations indicated a pressure gradient monotonically-weakening with increasing leeward distance, while the WT model predicted a leeward region of *weakly* adverse (or zero) pressure gradient, terminated downwind by an abrupt rise in pressure (so that the pressure-gradient is *not* monotonically decaying).

Measurements of mean pressure about a windbreak have been reported by Jacobs (1984), by Schmidt et al. (1995), and by Judd and Prendergast (1996). Jacobs investigated the case of a *solid* windbreak on level ground, but sampled the pressure only at $x/H = \pm 1$. Schmidt et al. provided a more detailed along-wind pressure profile at ground-level, but interpretation of their data is complicated by the small number of downwind sample-points, by non-uniformity of the surface (alfalfa upstream and wheat stubble downstream), by the thickness (order H) of the windbreak itself, and by their sampling strategy (5-min mean pressures derived from 5 samples, each averaged only by intake-line damping, which can be characterised by a time constant of order 10 sec). The aim of the present measurements, therefore, was to better determine the mean pressure field around the simplest type of shelter flow, a porous fence standing on level, uniform ground. For this purpose it suffices to measure pressure at ground level, because (below about $z = H$) the vertical gradient is much smaller than the horizontal gradient (see for example pressure contours calculated by WT) and by measuring at the ground one avoids the complication of having to provide static-pressure-intakes designed to reject the dynamic pressure signal ρV^2 ($\rho =$ air density; $V =$ instantaneous windspeed) induced by the probe itself. The experiment was commenced prior to the author's learning of the measurements by Judd and Prendergast, which coincidentally involved similar dimensionless parameters (H/z_0 , k_r), and which will be cited here in comparison with the present data.

2. Why is Measuring the Pressure Profile about a Fence Useful?

Correspondence (Wilson and Mooney, 1997; and reply by Takle and Wang) has not identified what specific difference(s) between the WT and W85 models explain(s) the faster leeward recovery given by WT. Wilson and Mooney implemented their own reconstruction of the WT model, but using Patankar's (1980) SIMPLE numerical method rather than the less-well documented WT gridpoint scheme. They thought the faster recovery hinged on restricting the height of the computational

* However, in their implementation of the WT model, Wilson and Mooney (1997) obtained a pressure field not essentially different from W85. In the following section we shall briefly review the discrepancies between the WT and W85 models, and the outcome of correspondence between the authors.

domain. But Wang and Takle, repeating simulations with their own code, did not find this to be true.

Differences between the W85 and WT representations of the drag due to the (thin) Bradley-Mulhearn fence may have contributed to differences between resulting simulations. Wilson and Mooney discussed these differences in parameterisation of the fence, which if nothing else suggest there is a need to develop appropriate criteria. In particular, to capture the narrow fence in their gridpoint model WT implemented an abrupt (stepwise) refinement of their grid in the region of the barrier, a procedure which (in general) merits concern in numerical fluid mechanics. It is not in principle essential that grid spacing ‘at’ the fence should match the physical thickness (W) of the fence. Details of the flow on that scale (W) probably are of no interest or importance. Indeed, to parameterise fence-drag by means of a bulk momentum sink (rather than by imposing no-slip/no-leak boundary conditions on a complex surface) implies that we forsake seeking details on that scale (W). What *is* important, for proper calculation of the flow in the sheltered region, is that the correct amount of momentum should be removed *near* the barrier. Under the control volume method of Patankar’s (1980) SIMPLE, used by W85, ‘near the barrier’ means ‘from the control volume spanning the fence’, a control volume whose width is free to be chosen quite irrespective of actual fence thickness, and in relation to one’s wish to resolve *important* flow gradients – important presumably meaning, significant on scales *much larger than* W . No discontinuity in gridlength need arise. Could the leeward ‘irregularities’ of the several WT pressure fields (for a thin fence) relate to this issue of grid-skew? Are they real? Or are they ‘computational’? That is the question the present experiment was intended to answer. And if there actually *is* a leeward pressure plateau behind a thin fence, contrary to simulations using SIMPLE, one must then suspect a problem with that enormously popular numerical method for these flow calculations.

What is the form of the ‘plateau’ feature sought in the observations? WT originally presented pressure *contours* (their Figure 5), which they discussed in the context of the Bradley-Mulhearn fence. Presumably their figure (5b; with $k_r = 2$) corresponds to the velocity field for the Bradley-Mulhearn data, and so was calculated using grid spacing $\Delta x = 0.05 H$ in the vicinity of the fence (see reply by Takle and Wang, 1997 to Wilson and Mooney, 1997). In any case those pressure contours showed qualitatively what Wang and Takle (1996a,b) later termed a ‘plateau’ in the near lee: the (adverse) pressure gradient did not monotonically relax with increasing downstream distance. Wang and Takle (1996a) gave pressure profiles for barriers of various widths $0.1 H \leq X \leq 10 H$ (simulated with gridlength $\Delta x = 0.1 H$) clearly showing this plateau, which was particularly marked for the narrowest (0.1 H) barrier. In their latest simulations of a narrow windbreak (reply to Wilson and Mooney), Takle and Wang (1997) reported not a ‘plateau’, but a region of weakly-adverse pressure-gradient.

Prolonged concern over differences between these models may not be justified, because the experimental data are not without uncertainty, and anyway it may be

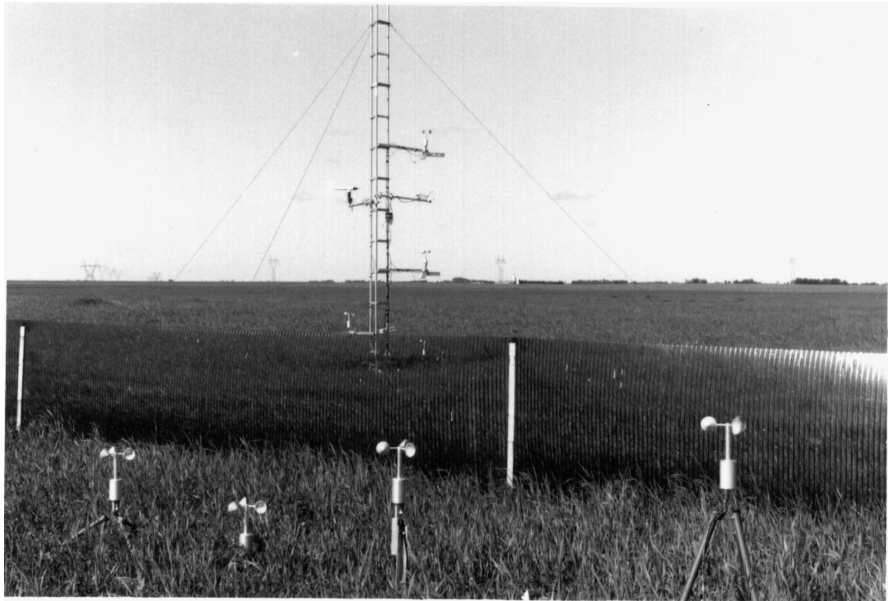


Figure 1. A view to the southwest at the site of the windbreak experiments, at Ellerslie, Alberta (height of the fence $H = 1.25$ m). The distant fenceline marks a road, at a distance of 0.6 km west from the fence. The photograph was taken on 12 June, 1996, on which date the cup anemometers were arranged to measure a vertical profile of the mean wind at $x/H = 2$ (given on Figure 8).

unrealistic to conceive of an exact, invariable ‘truth’ of the idealised flow. But on the other hand Wilson and Mooney emphasized that when *any* model of this type is applied to the very porous case ($k_r \ll 1$), a *very slow rate of leeward velocity-recovery occurs* (e.g., analytical solution by Wilson et al., 1990). Thus there remains a *possibility* that the present generation of closure models is deficient for windbreak flows. If such a deficiency does not exist, then perhaps it remains to clarify what pitfalls may exist in the computational representation of thin, localised momentum sinks.

3. Site Description and Measurement Procedure

The measurements were made during westerly winds, in a large field at the Ellerslie research farm of the University of Alberta (Figure 1). The field was quite level, its overall slope being less than about 1 or 2%. Some minor topographic undulations on long lengthscales (half-length $H_x \sim 50$ m) were visible, but their vertical/horizontal amplitude ratio H_z/H_x was around 1 : 200 or less, which is sufficiently small that topographically-induced pressure gradients should have been small compared to those due to the fence (Appendix A).

A plastic fence* of height $H = 1.25$ m and length $y = 55$ m = 44 H was erected in a NS orientation. To the west of the fence (upwind), level ground extended for 600m, to a gravel road. There were two intervals of measurements, June–July, 1996 ('summer') and October, 1996, ('autumn'). During the summer, when the windbreak stood in a canopy** of alfalfa and grass, the fetch of uniform upwind surface cover was reduced to 260 m (208 H), by a transition to immature wheat. During autumn, the windbreak (re-positioned after harvesting, ploughing and disking) stood on bare soil (roughness length $z_0 \approx 0.8$ cm; $H/z_0 \approx 160$; surface friction velocity $u_{*0}/\bar{u}_{0H} \approx 0.080$) and the uniform upwind fetch over the bare soil then extended to a distance of 370 m (296 H), at which point was encountered the now-mature wheat. During both periods of measurement, the surface downwind from the fence was identical to that upwind for a distance of at least 300 m.

To determine the state of the equilibrium surface-layer flow approaching the barrier (i.e., friction velocity u_{*0} , Obukhov length L , wind direction α , etc.), a 6 m lattice-type tower was erected 10 m (8 H) upwind from the midpoint of the fence. This carried Climet 011-B cup anemometers at heights: *Summer*, $z = 4.13, 2.16, 1.11, 0.69$ m; *Autumn*, $z = 3.56, 1.62, 0.65$ m. The tower also carried an RM Young windvane, aligned with respect to the fence to within approximately $\pm 2^\circ$ ($\bar{\alpha} = 0$ corresponds to mean wind direction normal to the fence); and a 1-dimensional sonic anemometer and fast thermocouple, measuring the mean vertical sensible heat flux density, Q_H . Averaging intervals of 30 min were used. Those intervals best matching the assumptions and restrictions of the numerical models are those with smallest mean and standard deviation of the wind direction ($\bar{\alpha}$, σ_α), and smallest Q_H . Signals were recorded on Campbell Scientific CR-7 and CR-21X dataloggers.

3.1. PRESSURE MEASUREMENTS

Though the local pressure changes induced in windbreak flow have great impact on the velocity field, they are nonetheless extremely small, and difficult to measure accurately. Twelve sample points were chosen, lying along a perpendicular line running through the midpoint of the fence. During most intervals, these were at $x/H = -4, -2, -1, 1, 2, 3, 4, 6, 8, 10, 12, 15$ (where $x/H = 0$ at the fence). However during some autumn measurements, locations $x/H = \frac{1}{4}, \frac{1}{2}, 1, 1\frac{1}{2}, 2, 3, 4, 5, 6, 8, 10, 15$ were used. These positions were chosen in the hope of resolving,

* Manufactured by the Tensar Corporation, who reported its porosity as 45%. The resistance coefficient (k_r) of this same plastic fence was measured earlier in conjunction with experiments reported by Argete and Wilson (1989). By placing a sample so as to block a wind tunnel flow, it was determined that $k_r = \Delta p / (\rho U^2) = 2.4$, where Δp is the pressure drop across the sample, U is the bulk windspeed, and ρ is the air density.

** Canopy height (h) increased over the measurement period, from about 45 cm to about 75 cm, but could be estimated only roughly, particularly late in June when the canopy was in two tiers, the grass high and the alfalfa low.

if present, the weak pressure-gradient region suggested by the flow simulations of Wang and Takle. Up to 24 sampling points could have been accommodated by the instrumentation, but due to the slow achievable sampling rate, restriction to twelve points was considered preferable. No attempt was made to capture the pressure drop $\bar{p}(0^+) - \bar{p}(0^-)$ across the fence, as the object of the experiment was not determination of the drag, or the resistance coefficient.

In all experiments prior to October 25, 1996, pressure at each of the twelve sample-points was transmitted (see Figure 2) down 15m of 1/8th inch I.D. Tygon tubing, then through a further length ($L_f = 2$ m) of finer ($d = 1/16$ th inch I.D.) Tygon tubing, and "held" in one of twelve large glass bottles (volume $V_b = 4$ litres). This constituted a low pass filter applied to the pressure signal, included because the available pressure transducer and multi-port valve could not be configured for rapid sampling. An analysis of the time constant τ_b of the tube and bottle filter is given in Appendix B. Theoretically, $\tau_b \approx 9$ sec, although a laboratory determination yielded a figure up to three times larger.

The 'tube & bottle' time constant is analogous to an electrical 'RC time constant' (flow resistance R , volumetric capacity C). It is in hindsight inadvisable to design a suitably-long averaging time constant τ_b by providing 'large C ' (4 litre bottle) and moderate R (only a 2 m length of the 1/16th" I.D. tubing); the same outcome can be attained without bottles, by simply using a much longer length of the fine tubing. The unforeseen disadvantage of using bottles to set the time constant was that their individual and differing rates of warming or cooling, in conjunction with the restriction of their venting through the field tubes, could give rise to pressure differences that overwhelmed those actually present between the sample points (i.e., thermally-induced pressure drifts between the bottles *could* mask those set up by the fence). To circumvent this problem, the bottles were buried in the soil to their necks, and shaded. On and after October 25, 1996, the tube-and-bottle filters were replaced by 15 m of 1/16th inch I.D. Tygon tubing, providing an effective time constant (characterising response at the outlet to step change in pressure at the inlet) of 7 sec.

At each sample point the conveying tube was taped loosely to a wire inserted in the soil, with the inlet facing down at about 1 cm above the soil level. While undoubtedly air motion near ground would have induced fluctuations in pressure, it is expected that their characteristic frequency was so high as to result in their having negligible effect on the damped pressure in the sample bottles. Jacobs (1984), measuring the mean pressure *within* the flow (heights up to 1.25 H), used special probes designed to eliminate contamination by interference of the flow with the intake.

Twenty-four short outlet tubes (1 m of 1/16th" I.D. Tygon) conducted the sample-bottle pressures (each bottle having two outlets) to a 24-inlet/single-outlet electrically-switched valve (Scanivalve), and sequentially forward to a differential pressure transducer (see below). The reference side of the transducer was constantly connected to the 'reference bottle' sampling the pressure at $x/H = 15$, thus all

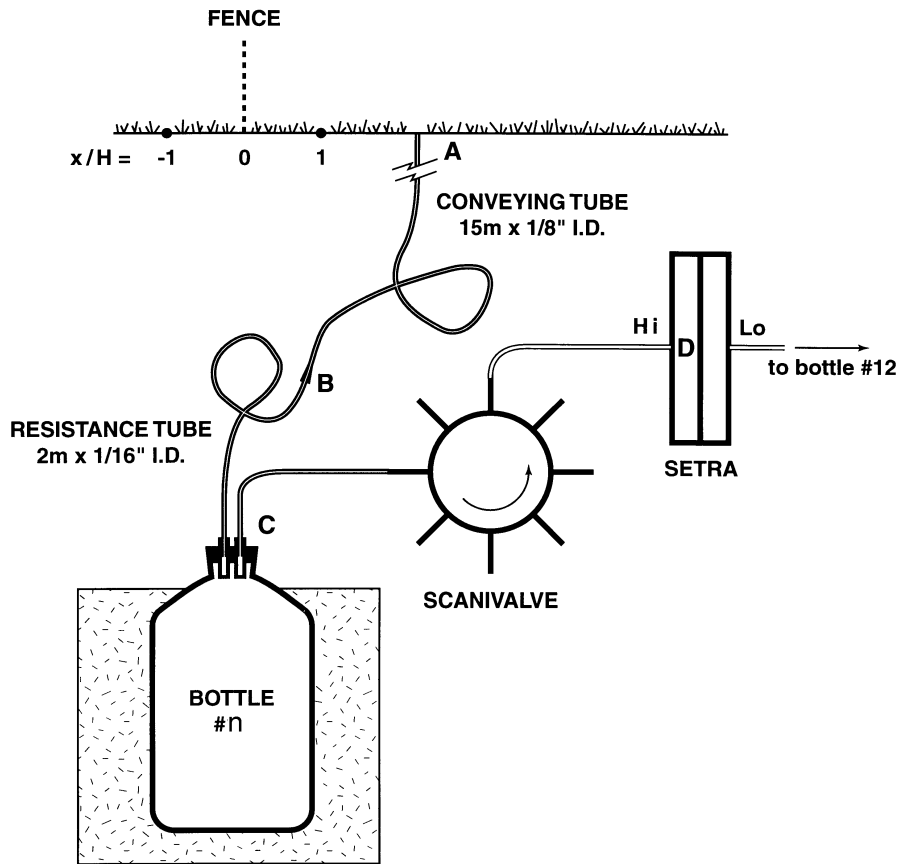


Figure 2. Schematic of equipment for pressure measurements. Pressure at inlet point A was conveyed down 15 m of 1/8th inch I.D. tubing to point B, then down 2 m of finer 1/16th inch I.D. tubing to the bottle. The tube and bottle filter (A-C) had time constant $\tau_b \approx 20$ sec. Surprisingly in view of the small volume along C-D, the 'outlet side' (i.e., C-D) had a time constant $\tau_{os} \approx 2$ sec, substantially longer than the pressure transducer alone, which had a time constant of only $\tau_{pt} = 0.64$ sec.

pressures cited are relative to pressure at that location. Note that one cannot assume the reference pressure was itself unperturbed by the fence.

The differential pressures were measured using a Setra Systems Inc. Model 264 transducer (Full Scale Range, $\pm 0.1''$ H₂O, i.e. ± 25 Pa). This was calibrated against a Dwyer Micropoint Manometer, and found to have sensitivity 9.81 Pa/volt (equalling the manufacturer's specification). Measurements of the step response (of the Setra itself) yielded an instrument time constant of $\tau_{pt} = 0.64$ s. Thus in measurements prior to October 11, 1996,* the valve was switched under control

* On which date it was discovered that the time constant of the transducer itself, $\tau_{pt} = 0.64$ s, was not the limiting time constant, but rather that response was limited by the time constant $\tau_{os} = 2.0$ s of the entire outlet side. Thereafter the switching interval was prolonged to 15 sec, obviating the need for lag correction of data collected on or after that date.

of the data-logger at intervals $\Delta t = 2.5$ sec, and the transducer was sampled at $t_D = 1.7$ sec after switching ($t_D =$ 'delay time'). This permitted, it was mistakenly believed (see below), virtually full response, and provided two readings per minute from each sample point (including two 'zero' readings, with the reference bottle connected to both sides of the transducer). Each reading was itself an average over an interval of order 20 sec, as set by the tube-and-bottle filter.

In the above design there had been *assumed* to be negligible volume in the 'measurement arm', i.e., between the outlet from the sample bottle and the transducer membrane (the pressure-signal path C-D on Figure 2). It was therefore considered unwarranted to be concerned with time lags other than due to the tube and bottle filter (τ_b) and the differential pressure transducer (Setra, τ_{pt}). In October however, when the distribution of the pressure intakes was rearranged to lie entirely on the leeward side, an inexplicably different mean pressure pattern was seen to result. It was an obvious hypothesis that the measurement arm (or 'outlet side', C-D) was responding too slowly in relation to the bottle-switching interval ($\Delta t = 2.5$ sec). This was confirmed when laboratory measurement of the step response of the 'outlet side' indicated a time constant of $\tau_{os} = 2.0 \pm 0.1$ s. Thus it was necessary to correct all data collected prior to 11 October, to compensate for the inadvertent smoothing. This was a straightforward and almost exact procedure (see Appendix 3). On and after that date, the switching interval was increased to $\Delta t = 15$ sec, with a delay of $t_D = 13$ sec between switching and measurement.

A Campbell Scientific datalogger (CR7) provided timing pulses which, through a relay, switched the sample valve. The latter provided a multi-position rotary electrical switch co-phased with the flow-valve. This was strung with resistors to provide a voltage divider, whose output was recorded in addition to the pressure-voltage, as a 'bottle-identifier' signal. The pressure transducer and the Scanivalve were housed in a waterproof fibreglass electrical box, beside the buried sample bottles.

The largest fence-induced pressure differences seen were of order 0.020-0.04'' H₂O (5-10 Pa), i.e., 1/5th-2/5th of the Full Scale Range of the transducer (e.g., Figure A1 shows an un-normalised pressure profile for a run during which the approach windspeed at fence height $\bar{u}_{0H} \approx 6$ m s⁻¹). Although the small pressure deviations were no surprise (in view of Wilson's 1985 simulations), considerable care was required in the measurements. The necessity of burying the filter-bottles to slow down their warming and cooling in response to environmental changes has been mentioned. Another pitfall was condensation in the tubing, resulting in formation of water column(s) inducing false windbreak-pressure signals. It was necessary to retrieve the tubing and the switching-valve daily, and flush them with dry air in the laboratory, prior to each new session of measurements. Before laying out the tubes to the field sample points, or after a day's measurements, if possible the system was checked by measuring 'zeros' with all inlets mounted together. As will be seen, the pressure data form a fairly self-consistent pattern, whether

measured with or without the bottles, and whether necessarily lag-corrected (fast sampling) or not (slow sampling).

3.2. ANALYSIS

A *C* program organised the logger output files, which contained the sequential pressure, bottle-identifier, and wind direction signals, as well as the half-hourly mean wind (and other) data. The correct bottle sequence was very occasionally broken (failure to switch), and such runs were easily corrected. Half-hour mean pressure in each bottle was calculated, from the (up to) sixty twelve-point alongwind profiles. Subsequently, if appropriate, the pressure data were lag-corrected to undo instrument smoothing, as described in Appendix C.

The analysis checked logger statistics of wind direction, also giving the maximum excursion of the wind away from normal, and the number of ‘reversals’ of wind direction ($|\bar{\alpha}| > 90^\circ$) during the interval. Only for runs during very oblique winds were reversals of the flow recorded (e.g., 29 June, run 14; $\bar{\alpha} = 52^\circ$, $\sigma_\alpha = 16^\circ$, four reversals).

For each run, the friction velocity was determined graphically from the mean wind profile on the upstream tower. Density was calculated daily, from measured local pressure (Environment Canada mercury barometer) and nominal temperature. Pressure data were normalised to permit comparison of data from differing micrometeorological conditions.

4. Numerical Simulations

In Section 4 the field observations of pressure and windspeed will be compared with numerical simulations, i.e., solutions of the mean momentum equations (plus the continuity equation, and a turbulence closure). For example the \bar{u} -momentum equation is:

$$\frac{\partial}{\partial x}(\bar{u}^2 + \sigma_u^2) + \frac{\partial}{\partial z}(\bar{u}\bar{w} + \overline{u'w'}) = -\frac{1}{\rho} \frac{\partial \bar{p}}{\partial x} - (c_d a + k_r \delta(x, 0) s(z, H)) |\bar{u}| \bar{u} \quad (1)$$

where σ_u is the standard deviation of the alongwind fluctuation (u'), and $\overline{u'w'}$ is the shear stress. Equation (1) differs from the form usual in micrometeorology only through the presence of the drag terms (momentum sinks) on the right hand side. Plant drag is parametrized using an effective drag coefficient c_d and leaf area density ‘ a ’ [m^{-1}]; while the windbreak is parametrized in terms of its resistance coefficient, and localised by the delta-function $\delta(x, 0)$ [m^{-1}] and the dimensionless step function $s(z, H)$.

4.1. FENCE ON BARE GROUND

Simulations by Wilson (1985; W85) used a standard numerical method, SIMPLE (Patankar, 1980, 1981); standard closures (including the second-order closure of

Launder et al. 1975, hereafter LRR); and a large computational domain ($-60 \leq x/H \leq 112$, $z/H \leq 47$). Solutions were subjected to several criteria of acceptability, including that the ‘whole domain’ \bar{u} -momentum balance should be correct to within 1% of the drag on the fence. The W85 model with second-order closure has been applied to simulate the present experiments, with only these alterations: specification of the present experimental conditions, ($H/z_0 = 160$, $k_r = 2.4$); re-zeroing of model pressure $\bar{p}_M(x/H, z/H)$ to match the field convention ($\bar{p} = 0$ at $x/H = 15$), by subtracting $\bar{p}_M(15, 0)$; and, refinement of grid resolution to ($\Delta x/H \geq 0.5$, $\Delta z/H \geq 0.125$).

4.2. FENCE STANDING IN A CANOPY: UNPERTURBED EDDY VISCOSITY SIMULATION (‘ K_0 CLOSURE’)

W85 showed that even if the eddy viscosity was assumed to be unperturbed by the windbreak, i.e., if the eddy viscosity was specified as $K(x, z) = K_0(z) = k_v u_{*0} z$ (where $k_v = 0.4$ is von Karman’s constant and u_{*0} is the friction velocity characterising the approach flow), simulations were in rather good agreement with the observed mean velocity field in the near lee. This was presumed to be a consequence of the flow near the fence being dominated by pressure-gradient forces and advection.

Carrying over this approach to the case of a fence within a canopy, one adopts self-consistent wind- and eddy-viscosity profiles for the upstream equilibrium flow, the eddy-viscosity profile $K_0(z)$ subsequently being imposed in a shelter-simulation along the entire alongwind axis, and the wind profile $\bar{u}_0(z)$ serving as an inflow boundary condition. Several such choices of paired mean wind and eddy-viscosity profiles are available. Simulations reported here adopt the simplest, which is associated with an exponential wind profile* within the canopy (unresolved by the present measurements). That is, if the eddy viscosity is specified as

$$K_0(z) = \lambda^2(z) \frac{\partial \bar{u}_0}{\partial z} \quad (2)$$

and the length scale as

$$\lambda(z) = \begin{cases} k_v(h-d) = \lambda_0, & z \leq h \\ k_v(z-d), & z > h \end{cases} \quad (3)$$

where d is the displacement height, then the equilibrium momentum budget

$$\frac{\partial}{\partial z} \left(K_0 \frac{\partial \bar{u}_0}{\partial z} \right) = c_d a \bar{u}_0^2 \quad (4)$$

* Similar results follow from choosing Cowan’s (1968) hyperbolic-sine wind profile, which corresponds to the specification $K = \lambda \bar{u}(z)$ within the canopy, with $\lambda = \text{const}$.

implies an (analytical) equilibrium wind profile:

$$\bar{u}_0^A(z) = \begin{cases} \bar{u}_{0h} \exp\left(\frac{\gamma}{\lambda_0} \left(\frac{z}{h} - 1\right)\right), & z \leq h \\ \bar{u}_{0h} + \frac{u_{*0}}{k_v} \ln\left(\frac{z-d}{h-d}\right), & z > h \end{cases} \quad (5)$$

The parameters are inter-related according to:

$$\gamma = \frac{u_{*0}}{\bar{u}_0(h)} \quad (6)$$

$$c_d a = \frac{2\gamma^3 h}{\lambda_0}. \quad (7)$$

However, rather than adopt Equation (5), in order to provide an inflow profile *exactly* in equilibrium with the eddy viscosity implied by Equations (2,3), and to enforce the no-slip condition at ground (whereas Equation (5) implies slip), the momentum Equation (4) was discretized and solved numerically, to obtain the (discrete) inflow profile $\bar{u}_0(z)$.

The key parameters for a windbreak standing in a canopy are: d/h , H/h , $c_d a h$, and k_v . Values of the first three of these are somewhat uncertain, and were estimated as follows: friction velocity u_{*0} and displacement height d were determined graphically from the mean wind profile; while a range for the canopy height h was assessed from a sample of measurements. This established ranges for H/h and d/h , the latter implying a range for other parameters:

11–12 June, 1996: $d = 0.2 \pm 0.02$ m; $h = 0.45 \pm 0.05$ m; $0.4 \leq d/h \leq 0.5$; $2.5 \leq H/h \leq 3.1$; and $\gamma \approx 0.28$.

29 June, 1996: $d = 0.4 \pm 0.02$ m; $h = 0.75 \pm 0.15$ m (two-tier canopy; alfalfa height was assessed as 0.5–0.7 m, and grass height as 0.8–1.0 m); $0.45 \leq d/h \leq 0.65$; $1.4 \leq H/h \leq 2.1$; $\gamma \approx 0.35$.

Numerical procedures for simulating the windbreak-in-canopy case differed slightly from W85 (similar work subsequent to these simulations has established that the differences are unimportant). The lowest \bar{u} -gridpoint was set at the ground, to allow imposition of the no-slip condition within the canopy (one must otherwise adopt a ‘wall-layer’ relationship at the canopy floor between surface shear stress and velocity). Gradients in turbulent velocity variances were entirely neglected. Finally, a high-resolution non-uniform grid, having $\Delta x/H \geq 0.2$, $\Delta z/H \geq 0.065$, covered a domain ($-60 \leq x/H \leq 120$, $z/H \leq 40$).

5. Results

In addition to selection criteria with respect to mean wind direction, in order to avoid ‘noisy’ estimators of the normalised mean pressure field ($\bar{p}/\rho u_{*0}^2$) it was

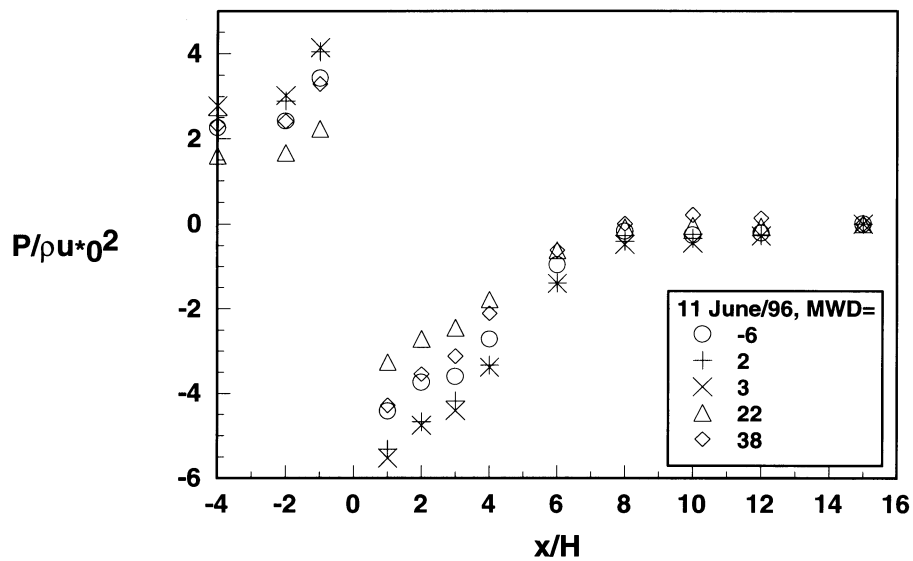


Figure 3a. Horizontal profiles of normalised ground level pressure $\bar{p}/\rho u_*^2$ versus x/H , for a range of mean wind directions (MWD). Windbreak standing in canopy.

necessary to reject data from periods of light winds, during which time the pressure disturbance due to the windbreak drag $k_r \bar{u}^2$ is reduced, but the error level (eg. due to unevenly-drifting bottle temperatures) is unaffected. Table I summarises the atmospheric conditions during the pressure measurements, for all runs reported in this paper. Table II gives the mean pressure profiles, for runs with the fence on bare soil. Data collected with switching interval $\Delta t = 2.5$ s have been 'lag-corrected' as indicated in Appendix C.

5.1. MEAN PRESSURE VERSUS OBLIQUITY OF FLOW INCIDENCE

Figures 3a,b show normalised pressure profiles for several 30-min periods on June 11, 1996, and on October 7, 1996, on both of which days mean wind direction ranged from nearly-perpendicular out to 30 or 40°. Surprisingly, across that range of obliquity of the wind, there was only modest (and not completely systematic) alteration of the pressure field. While on Figure 3a greater amplitudes of the pressure profile clearly occurred for smaller $|\bar{\alpha}|$, on Figure 3b such a systematic stratification with respect to $|\bar{\alpha}|$ is not evident. No reversals of the wind direction were recorded during any of these runs. However for obliquity as large as $\bar{\alpha} > 50^\circ$, in which cases reverse flow sometimes occurred, the pressure amplitude was observed to have decayed by a factor of order ten.

Judd and Prendergast (1996) also noted this relative insensitivity of the pressure field (but not the wind field) to flow obliquity. Therefore runs with $|\bar{\alpha}|$ as large

Table I
 Micrometeorological parameters during observations of mean pressure about a porous fence at Ellerslie

Date	Interval	Run #	w^* [m/s]	M.W.D.	S.D.W.D.	$Q_H, W m^{-2}$	d [m]	Smp. int. [s]	Dnsy kg/m^3
June 11, 1996	1601-1630	3	0.65	-6	19	-15	0.2	2.5	1.13
June 11	1631-1700	4	0.75	2	14	-23	0.2	2.5	
June 11	1731-1800	6	0.82	2	15	-33	0.2	2.5	
June 11	1801-1830	7	0.72	22	14	-9	0.2	2.5	
June 11	1831-1900	8	0.85	38	16	-12	0.2	2.5	
June 29	1101-1130	1	0.67	29	13	49	0.4	2.5	1.11
June 29	1131-1200	2	0.65	28	17	65	0.4	2.5	
June 29	1201-1230	3	0.6	22	17	-5	0.4	2.5	
June 29	1331-1400	6	0.59	7	15	60	0.4	2.5	
June 29	1531-1600	10	0.54	13	19	43	0.4	2.5	
June 29	1731-1800	14	0.39	52	16	na	0.4	2.5	
October 7	1201-1230	1	0.28	-31	10	54	0	2.5	
October 7	1231-1300	2	0.31	-10	17	110	0	2.5	1.11
October 7	1301-1330	3	0.44	2	13	136	0	2.5	
October 7	1331-1400	4	0.38	-7	15	84	0	2.5	
October 7	1401-1430	5	0.4	-7	13	50	0	2.5	
October 7	1531-1600	8	0.31	-22	20	-4	0	2.5	
October 11	1601-1630	13	0.27	0	13	na	0	15	1.14
October 11	1631-1700	14	0.31	-15	10	na	0	15	
October 11	1701-1730	15	0.27	-13	8	na	0	15	
October 11	1731-1800	16	0.27	-11	8	na	0	15	
October 25	1231-1300	8	0.44	25	12	na	0	15	1.17
October 25	1301-1330	9	0.46	25	11	na	0	15	1.17
October 25	1331-1400	10	0.46	25	11	na	0	15	1.17
October 25	1401-1430	11	0.48	27	11	na	0	15	1.17
October 25	1231-1430	8, ..., 11	0.46	26	11			15	1.17
October 25	1001-1700	2, ..., 16	0.47	30	11		0	15	1.17

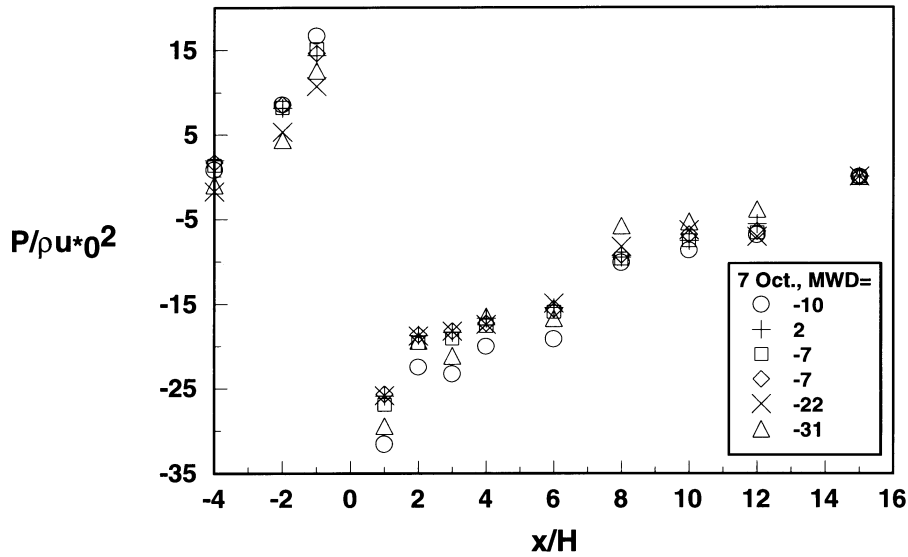


Figure 3b. Horizontal profile of normalised ground level pressure $\bar{p}/\rho u_{*0}^2$ versus x/H , for a range of mean wind directions (MWD). Windbreak on bare soil.

as about 25° will be considered as representing the mean pressure in ‘normally-incident’ flow.

5.2. MEAN PRESSURE FOR NORMALLY-INCIDENT FLOW

5.2.1. Bare Ground Versus Canopy

Figure 4 gives a sample of the observed profiles* of ground-level pressure during periods when $|\bar{\alpha}| \leq 25^\circ$, both within the alfalfa canopy and over bare soil. In order to compare these summer and autumn data, the approach velocity \bar{u}_{0H} is more suitable than u_{*0} as normalising velocity scale, for the pressure drop across the barrier is of order $\Delta\bar{p} = k_r \rho \bar{u}_{0H}^2$, but the ratio u_{*0}/\bar{u}_{0H} differs between the bare and vegetated surfaces. Over bare soil the drag on the exposed fence is larger with respect to the surface shear stress than is the case for the summer measurements. It is reassuring that the data of 11 and 25 October, obtained without need for lag-correction, show no systematic difference from the earlier data.**

* Where mean wind direction was essentially constant over several runs, data have been averaged to provide a single profile.

** On October 7 and October 11 the switching interval was $\Delta t = 15$ sec, with a delay between switching and sampling of $t_D = 13$ sec. Furthermore on October 25, observations were made without use of the tube- and-bottle filters, relying only on the averaging (time constant 7 sec) inherent in using 15 m long 1/16th inch I.D. conveying tubes.

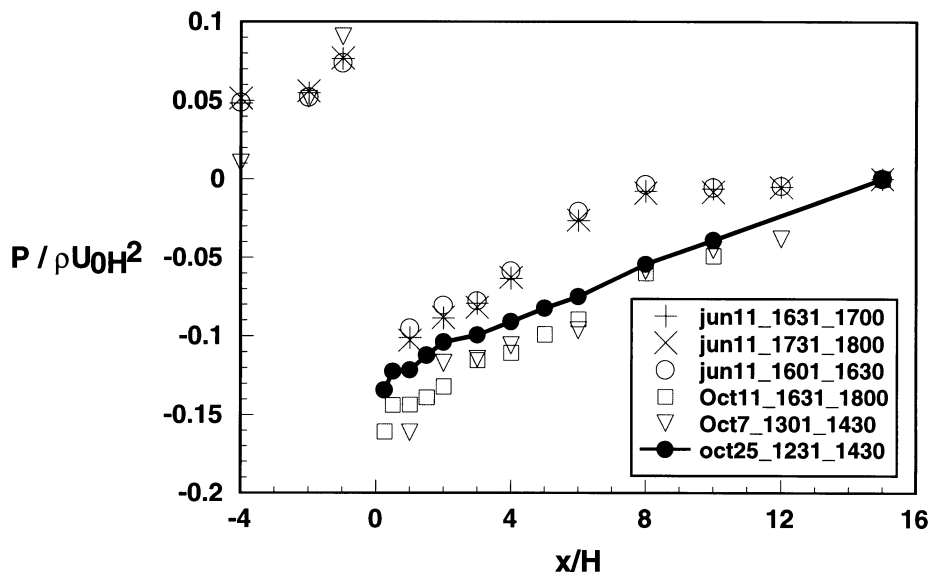


Figure 4. Comparing horizontal profiles of normalised ground level pressure $\bar{p}/\rho\bar{u}_{0H}^2$ during periods of near perpendicular mean wind ($\bar{\alpha} < 25^\circ$), for a windbreak within an alfalfa canopy (June, 1996), and a windbreak on bare soil (October, 96).

5.2.2. Fence on Bare Ground

Figures 5a,b,c give the individual pressure profiles, scaled on the friction velocity, for three days of measurements over the bare soil (u_{*0}/\bar{u}_{0H} is approximately constant across these data, but u_{*0} was adopted for the normalisation, due to its being the traditional surface-layer velocity scale). Measurement procedure varied over these days as earlier discussed, and positions of the sample-points were concentrated in the near lee on October 11 and 25. Minimum pressure and strongest pressure-gradient always occurred at the leeward sampling point closest to the windbreak. Only on October 7 did the pressure profiles show sign of a reduced pressure gradient over the range $2 \leq x/H \leq 6$. Potentially this is evidence for the 'plateau' feature diagnosed by Wang and Takle (1995) in their simulations. However given the susceptibility of the measurements to systematic error, it is *probably* justified to assume the pattern – seen October 7 but not on the later two days – is simply erroneous. The very satisfactory 'zeroes' profile, given on Figure C1 for October 7, was taken late in the afternoon – and does not rule out systematic error earlier in the day. In this context (judging whether a leeward plateau exists), greatest weight should be given to the profiles of October 25 (Figure 5c), obtained without using the pressure-averaging bottles, and therefore less vulnerable to error.

If one assumed the data to be free of systematic errors, one could argue that further averaging across all runs provides better representation of the 'true' pressure profile than the individual 30-min mean profiles. On Figure 6 that 'bulked' profile (i.e., average of all the bare-soil profiles of Table II) and the corresponding *range* are

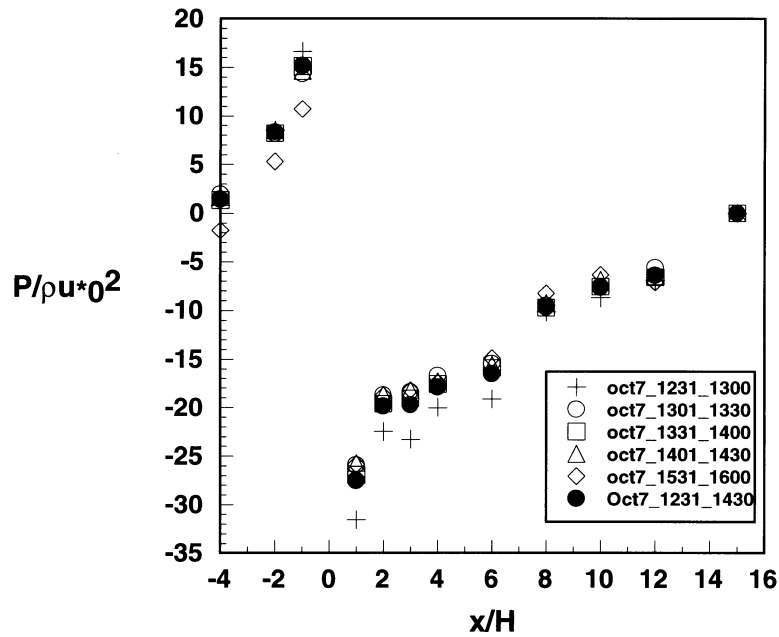


Figure 5a. Horizontal profile of normalised ground level pressure $\bar{p}/\rho u_{z_0}^2$ versus x/H , during periods of near perpendicular mean wind ($\bar{\alpha} \leq 22^\circ$), for cases of the windbreak standing on bare soil. October 7, 1996. Mean wind directions (in order given by legend) were: $\bar{\alpha} = -31, -10, 2, -7, -7, -22$ degrees. For the composite 120 min interval, $(\bar{\alpha}, \sigma_\alpha) = (-6^\circ, 15^\circ)$.

plotted, in comparison with the data of Judd and Prendergast (1996; hereafter JP), and with computed pressure fields. It would be appropriate to plot the (far smaller) standard-error bars in place of range if one *knew* that systematic (instrumentation) errors did not occur. But in view of the experimental difficulties alluded to, this is not a reasonable supposition, and so one must live with an uncertainty only modestly smaller than indicated by the range bars. In that case, and invoking ‘Ockham’s Razor’, there is no basis for considering the pressure recovery in the Ellerslie experiments to be other than monotonic, nor is there convincing evidence of a weak pressure-gradient region.

Judd and Prendergast measured thirty consecutive 15-min profiles of pressure at $z/H = 0.55$, during rather steady, nearly normally-incident winds, about a fence standing in pasture ($H = 1.92$ m, $k_r \approx 3$, $z_0 \approx 0.012$ m, $H/z_0 \approx 160$). They used probes (pressure-line intake ports) designed to reject self-induced dynamic pressure rise ($\approx \rho V^2$), and saw no evidence of failure to do so; but one should bear in mind that the probes were exposed to unequal mean and turbulent windspeeds, so any response to ρV^2 would alter the apparent static pressure profile. The JP data given on Figure 6 have been re-zeroed to make their profile coincide at $x/H = 10$ with the Ellerslie profile. As vertical pressure gradients near ground behind a fence are small, these data are directly comparable with the Ellerslie measurements.

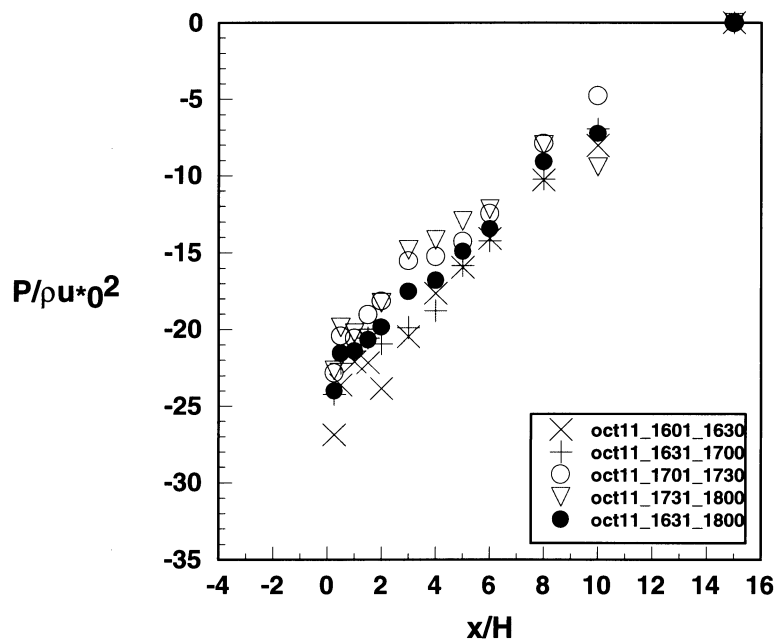


Figure 5b. Horizontal profile of normalised ground level pressure $\bar{p}/\rho u_{*0}^2$ versus x/H , during periods of near perpendicular mean wind ($\bar{\alpha} \leq 15^\circ$), for cases of the windbreak standing on bare soil. October 11, 1996. Mean wind directions (in order given by legend) were: $\bar{\alpha} = 0, -15, -13, -11$ degrees. For the composite 90-min interval, $(\bar{\alpha}, \sigma_\alpha = (-12^\circ, 8^\circ))$.

The thirty JP profiles were remarkably consistent; at each measurement point, the standard deviation over the thirty estimates of $\Delta\bar{p}/\rho u_{*0}^2$ was only of order 1 unit. The weak pressure-gradient zone defined by the JP observations at $x/H = 3, 5$ could be termed a 'plateau', but if real, whether it corresponds to the plateau of the WT model is unclear. Wang and Takle (1996a; Figure 5, $W = 0.1 H$) show a plateau encompassing $1 \leq x/H \leq 6$, whereas if one judges that the JP data imply a 'real' plateau at $3 \leq x/H \leq 5$, one must to be consistent, also judge that the plateau is not quite like that of the simulation – because it does not commence at $x/H = 1$. In a more recent simulation (reply to Wilson and Mooney, 1997), WT show a region of weakly adverse pressure-gradient, lying at close to the minimum pressure, and spanning roughly $1 \leq x/H \leq 6$; but the JP feature lies about half-way between the minimum and background pressures.

On Figure 6 the model pressure profile deviates seriously from the (bulked) observations both upstream from the fence, and around $x/H = 10$. No comment is offered, other than to note that it would require a quite *irregular* model profile to match all the data. A good simulation of the magnitude $\Delta\bar{p}$ of the pressure drop across the fence (not captured by the measurements, the closest upstream sample location being $x/H = -1$) is assured, provided modelled windspeed 'at' the fence is accurate.

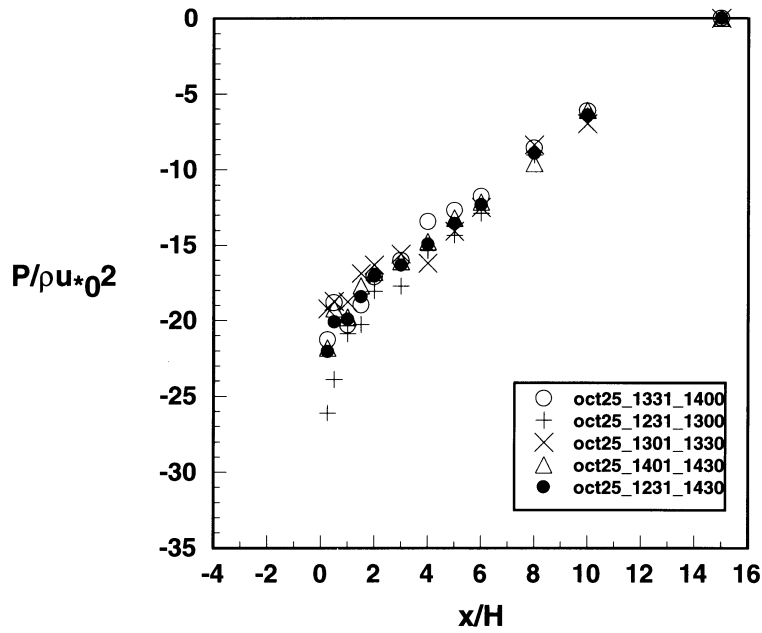


Figure 5c. Horizontal profile of normalised ground level pressure $\bar{p}/\rho u_{z_0}^2$ versus x/H , during periods of near perpendicular mean wind ($\bar{\alpha} \leq 27^\circ$), for cases of the windbreak standing on bare soil. October 25, 1996. Mean wind directions (in order given by legend) were: $\bar{\alpha} = 25, 25, 25, 27$ degrees. For the composite 120-min interval, $(\bar{\alpha}, \sigma_\alpha) = (26^\circ, 11^\circ)$. Note: data on this occasion were measured without using the pressure-averaging bottles.

The numerical model assigns no role to the standard deviation of wind direction. To investigate the possibility that swinging wind direction might have had principally the effect of altering the ‘effective fetch’ at any fixed measurement location (x), in such a way as to result in the observed mean pressure being effectively a ‘mixed-up’ version of the ideal (model) profile $\bar{p}_m(x)$, the following smoothed model profile was calculated:

$$\langle \bar{p}_m(x) \rangle = \int_{-\pi/2}^{\pi/2} \bar{p}_m \left(\frac{x}{\cos \alpha} \right) g(\alpha) d\alpha \tag{8}$$

where $x/\cos(\alpha)$ is the effective fetch for instantaneous wind direction α , and

$$g(\alpha) = \frac{1}{\sqrt{2\pi}\sigma_\alpha} \exp \left(-\frac{\alpha^2}{2\sigma_\alpha^2} \right) \tag{9}$$

is an approximation to the probability density function for wind direction. The resulting smoothed model profile differed negligibly from that given on Figure 6.

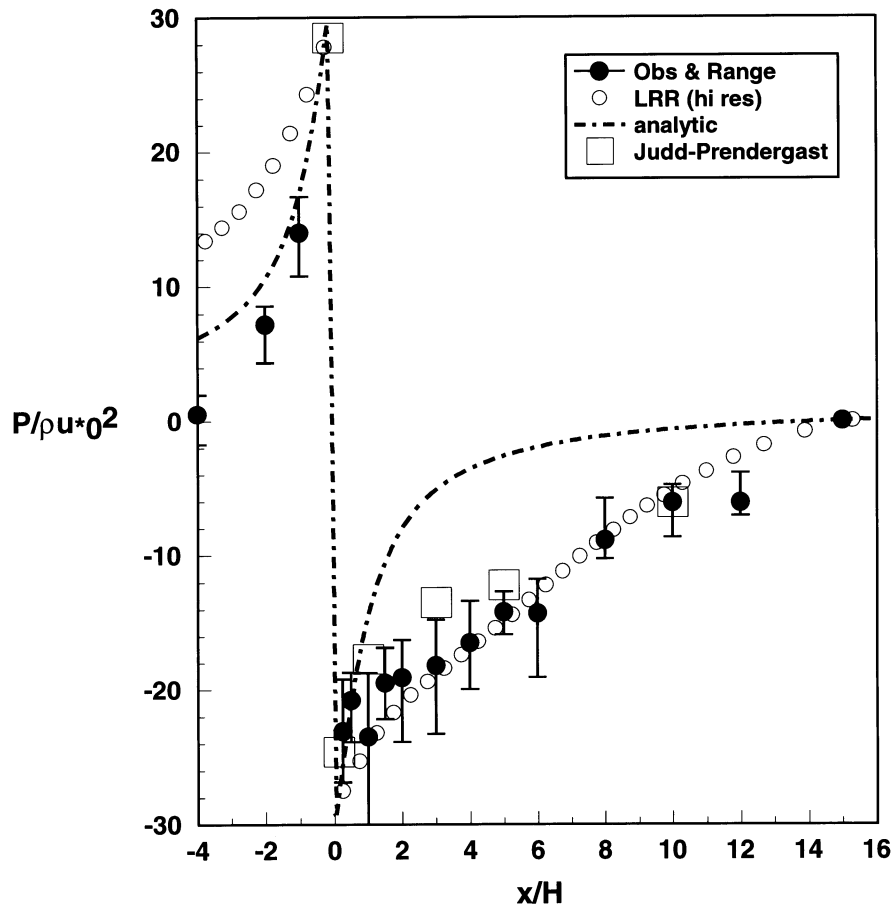


Figure 6. Overall-average profile (●, and range) of normalised ground level pressure $\bar{p}/\rho u_{*0}^2$ during periods of near perpendicular mean wind ($\bar{\alpha} < 25^\circ$), for cases of the windbreak standing on bare soil. Also shown (□) are similar observations made by Judd and Prendergast (1996) at height $z/H = 0.55$; a simulation (○) using the model of Wilson (1985); and the analytical profile of Wilson et al. (1990).

Also plotted on Figure 6 for comparison with the observations is an analytical pressure profile*

$$\frac{\bar{p}(x, 0) - \bar{p}(15H, 0)}{\rho u_{*0}^2} = 20 \left(\arctan \left(\frac{1}{15} \right) - \arctan \left(\frac{H}{x} \right) \right) \quad (10)$$

taken from Wilson et al. (1990; the amplitude factor, 20, is arbitrary). Foreknowledge of the pressure profile *could* provide the basis for a simplified shelter model (the known pressure simply being *imposed* in the streamwise momentum

* Valid for the flow of homogeneous turbulence through a very porous barrier standing on a free-slip wall (no shear in the approach flow), with the Reynolds stress neglected.

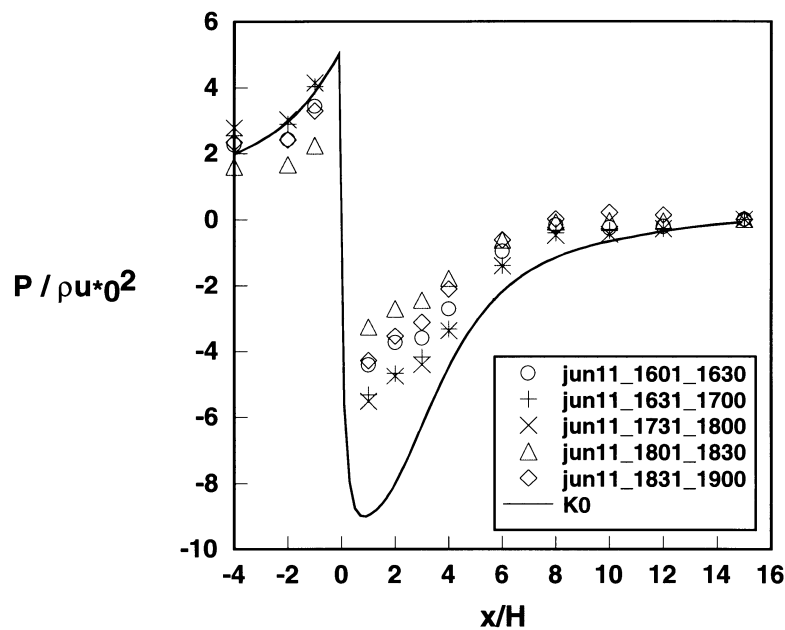


Figure 7a. Horizontal profile of normalised ground level pressure $\bar{p}/\rho u_*^2$ versus x/H , during periods of near perpendicular mean wind ($\bar{\alpha} < 25^\circ$), for cases of the windbreak standing within a plant canopy (11 June, 1996). Also shown, a simulation (line, 'K0') based on unperturbed eddy viscosity, with parameters: $k_r = 2.4$, $H/h = 2.7$, $d/h = 0.5$, $\lambda_0/h = 0.2$, $\bar{u}_{T4}/u_* = 10.62$, which imply $\gamma = 0.28$ and $c_d a h = 0.22$. Canopy height h , not determined directly, was the only uncertain parameter.

equation). But clearly this analytical pressure profile is quite wrong in form when k_r is not small. It contains no length scale other than the barrier height H , and cannot be readjusted to match the observed profile simply by alteration of the scale factor (which is related to the actual windspeed at the fence, assumed unperturbed in the derivation of the formula).

5.2.3. Fence in a Canopy

Figures 3a,b indicated the considerable effect on the pressure step through a windbreak when it is immersed in a canopy. Figures 7a,b compare the in-canopy data with a numerical simulation. According to the simulation, the point of minimum pressure lies somewhat *downstream* from the fence, rather than 'on' the back of the fence ($x = 0^+$). That aspect is not evident in the 11 June data ($d = 0.2$ m); however by 29 June, when canopy height had increased ($d = 0.4$ m), pressure at $x/H = 2$ was slightly lower than at $x/H = 1$. Also evident on June 29 was a slight *over-recovery* of mean pressure, over the region 6–10 H .

Finally, Jacobs (1984) reported that the pressure increment on the front of his (solid) fence was much smaller than the pressure depression behind. The present observations should not be considered as confirming that finding, because it is unlikely that the reference pressure at $x/H = 15$ represents the equilibrium pres-

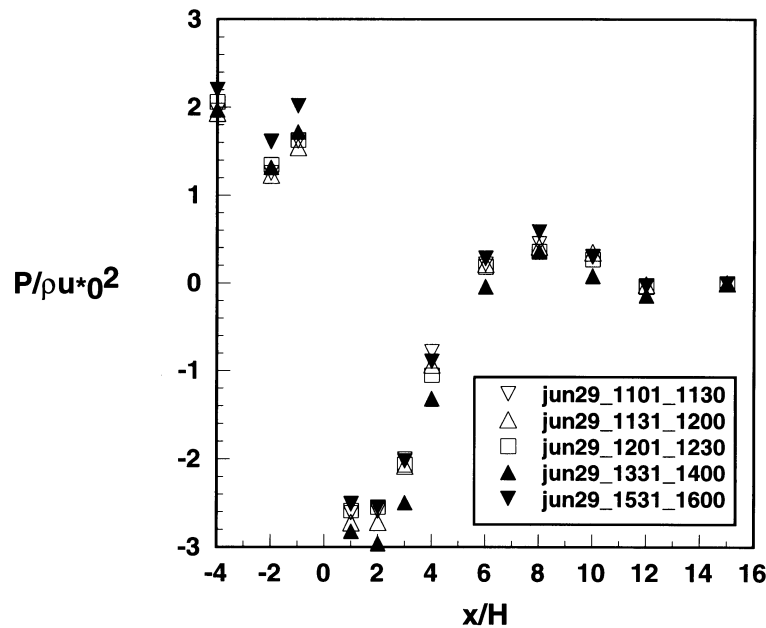


Figure 7b. Horizontal profile of normalised ground level pressure $\bar{p}/\rho u_{*0}^2$ versus x/H , during periods of near perpendicular mean wind ($\bar{\alpha} < 25^\circ$), for cases of the windbreak standing within a plant canopy (29 June, 1996).

sure. For example according to the simulation giving the pressure profile shown on Figure 6, relative to the mean pressure at $x/H = 15$ the mean pressures at $x/H = (-45, 100)$ are about $\bar{p} = (+4, +3) \rho u_{*0}^2$. Readjustment of the pressure-zero by -4 units in for example, Figure 5a, would result in the front-side pressure rise being approximately equal and opposite to the lee-side depression.

5.2.4. Mean Wind Reduction

During the summer measurements, up to five cup anemometers were set in the lee of the fence, configured to provide a vertical or horizontal profile of the mean wind. Figures 8a,b give the measured mean velocity profiles for 11–12 June, in comparison with a simulation assuming the eddy viscosity is unperturbed. Bearing in mind that the wind within the canopy was not resolved, and that the unobserved detail of the approach profile (approximated in the model by the solution of Equations (2)–(4)) certainly impacts on the windbreak drag, the model results are quite satisfactory: as for a fence on bare ground, the assumption of an unperturbed eddy viscosity suffices to provide a qualitative picture of the mean wind reduction. In the immediate lee of the fence, the simulation suggests the mean windspeed deep in the canopy is *increased*, which agrees with the measurements of Judd et al. (1996).

Figure 9 collects horizontal profiles of the mean wind, observed on the afternoon of 29 June, 1996, during which there occurred a wide variation in the mean wind

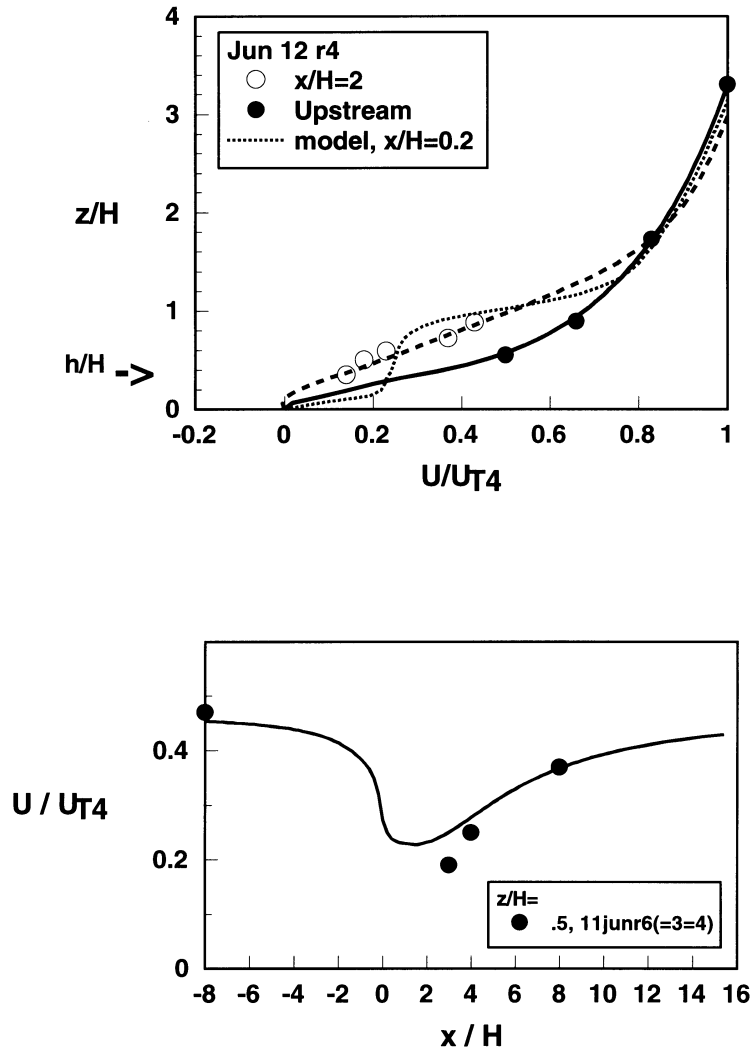


Figure 8a. (a) Vertical profiles of the normalised mean windspeed \bar{u}/\bar{u}_{T4} (where \bar{u}_{T4} is the windspeed at $z = 4.13$ m on the upstream tower), observed on 12 June, 1996 upstream (●) and downstream (○) from a windbreak in a canopy. The simulation (solid line, $x/H = -\infty$; dotted line, $x/H = 0.2$; dashed line, $x/H = 2$) uses the K_0 closure, with parameters: $H/h = 2.7$, $d/h = 0.5$, $\gamma = 0.28$, $c_d a h = 0.22$. Note the *speedup* immediately behind the fence, deep in the canopy. (b) Horizontal profile of the normalised mean windspeed \bar{u}/\bar{u}_{T4} (where \bar{u}_{T4} is the windspeed at $z = 4.13$ m on the upstream tower), observed (●) at height $z/H = \frac{1}{2}$ on 11 June, 1996 about a windbreak in a canopy. Simulation (solid line) uses the K_0 closure, with parameters: $H/h = 2.7$, $d/h = 0.5$, $\gamma = 0.28$, $c_d a h = 0.22$.

direction. In the near lee there was (systematically, at $x/H = 4, 6$) greater wind reduction for more-nearly perpendicular incidence of the wind, with lesser wind reduction (less effective shelter) during oblique winds. A slight over-recovery of the wind in the far lee occurred during oblique winds.

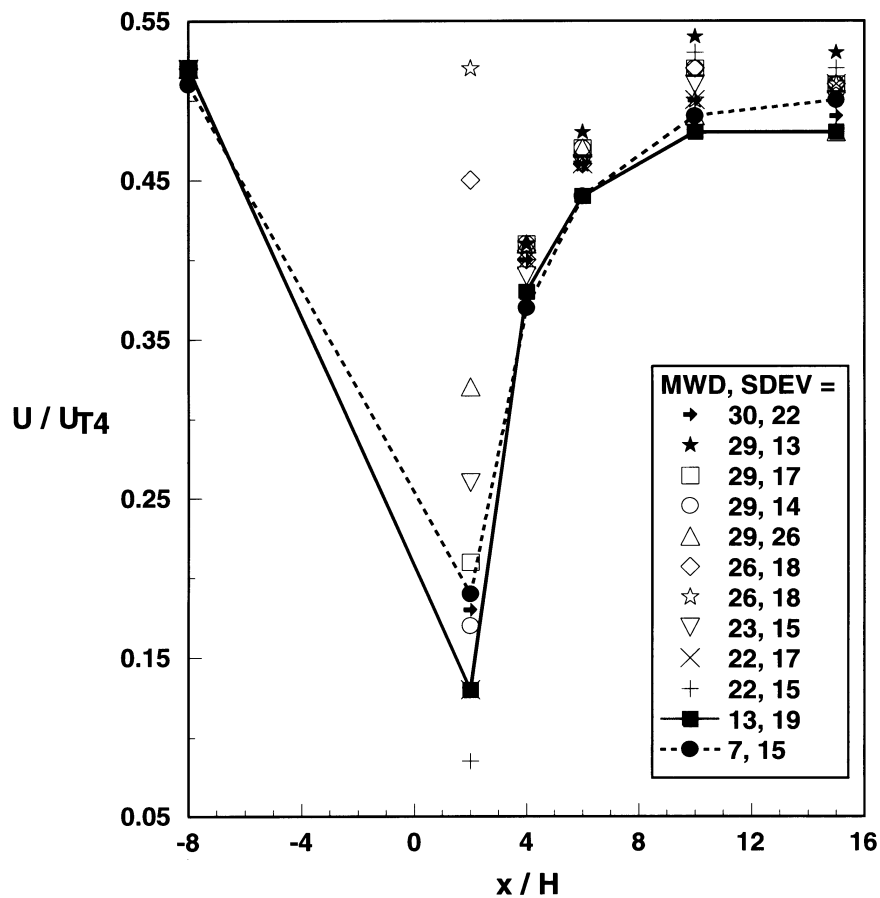


Figure 9. Horizontal profiles of the normalised mean windspeed at height $z/H = 0.73$, over a range of mean wind directions (MWD) and standard deviations (SDEV) on 29 June, 1996.

A surprising aspect of Figure 9 is the spread in measured windspeed at $x/H = 2$. At the commencement of the day's measurements it was noted that this anemometer, whose cable was stretched to the limit, was giving 'no count'. That problem having been resolved, the anemometer subsequently gave readings sometimes according with a normal wind reduction curve, and sometimes indicating little or no speed reduction at all! It is hard to explain a cup anemometer of this type (single-slot light-chopper mechanism) giving *too many* counts, except possibly due to cup stalling – which did not happen on this windy afternoon. Was this anemometer at the margin of a jet – sometimes subjected to strong wind, sometimes not? The data have been included because, *if correct*, they suggest the following point. The 'ideal flow' that the models envisage may be difficult to find in practice. Perhaps it is unrealistic to envisage a body of 'perfect' field data as criterion for the corresponding 'ideal' models.

6. Conclusions

The pressure field in a shelter flow is of no *direct* practical interest – plants do not respond, nor soils erode the less or the more, because mean total pressure has risen or dropped by a few Pascals. But pressure exerts an important influence *indirectly*, through its impact on the velocity field, so accurate calculation of the pressure field is demanded in theories of shelter flow.

The experiment reported here determined the (30 min) mean ground-level pressure profile for an ideal type of shelter flow, namely, the disturbance of the neutral surface layer (parameters: u_{*0} , z_0) by long, very thin, porous fence (H , k_r), with the mean wind at nearly-perpendicular incidence ($|\bar{\alpha}| < 25^\circ$). Data from such flows constitute the best basis at present for judging the skill of theories and simulations of windbreak flow, and the provision (here) of pressure data augments the available criteria against which models can be judged. Considering the run-run variability in the observed pressure profiles and the attendant uncertainty, the simplest interpretation of the Ellerslie data is that the pressure-gradient in the lee of a windbreak on bare soil decreases monotonically with increasing downwind distance. This agrees qualitatively with shelter simulations reported by Wilson (1985), but not with simulations by Wang and Takle (1995, 1996a,b; and the Takle and Wang, 1997, reply to Wilson and Mooney, 1997). On the other hand *some* of the profiles (October 7) collected at Ellerslie could be argued to indicate a pressure plateau resembling (some of the) WT model profiles. The Judd-Prendergast (1996) data also reveal such a feature. Therefore it cannot be categorically stated that there is not, in the near lee of a very thin fence, some sort of ‘plateau’ or weak pressure gradient region, such as Wang and Takle have suggested. Hopefully, subsequent work (preferably in the wind tunnel, to eliminate confounding factors) may resolve the question.

Some clarification of the grid- and closure-dependence of model pressure profiles is due. Pressure profiles calculated by Wilson (1985) varied somewhat according to the turbulence closure he adopted, and with grid resolution. In the absence of any pressure observations, and viewing pressure on the ‘whole domain’ scale ($|x/H| \leq 80$), and bearing in mind that pressure *gradient* (not absolute pressure) is the important property – it was unwarranted at that time to focus on minor variations between simulations. Now – with field data available, and disagreement reported between different models – finer discrimination is appropriate. The SIMPLE numerical method, as applied by W85, does not provide, for given fence and flow parameters, a *unique* pressure profile. Likewise, there is not just *one*, unique (and different from W85) Wang–Takle profile. That said, *no* windbreak simulation by the author has *ever* produced a plateau feature like those identified for thin windbreaks by Wang and Takle (1996a). In this sense, a dichotomy exists between the two (W85, WT) numerical approaches. And if further observations prove the WT plateau *does* exist – as a dynamically-significant feature, not a mere wiggle in the \bar{p} -profile – then it may follow that there is a previously unknown problem with the popular SIMPLE algorithm.

But do these differences between numerical shelter models matter? After all, neither represents ‘reality’, for many simplifications have been made. The assumption of two-dimensionality of the mean properties ($\bar{\alpha} = 0$, $\bar{v} = 0$) is potentially legitimate, though seldom true. More fundamental shortcomings are that the models assign no role for wind direction fluctuations; they invoke an idealised description of the barrier (H , k_r) that neglects details such as for example, deflection of the fence itself by the wind; and perhaps most seriously, they introduce closure approximations. Real windbreak flows, even contrived ones such as this, are rich with detail: flexing of the windbreak, spatially-varying soil roughness, undulations of topography, birds visiting anemometers, and so on. In view of all this it is unreasonable to *expect* perfect agreement, of field data and the simulations of numerical fluid dynamics. How could field data, even if perfectly measured, be completely site- and occasion-invariant?

For all that, there is reason for concern *if* a model (W85 *and/or* WT) is inconsistent *qualitatively* with the measured flow it represents. Further, more careful measurements of the simplest shelter flows may help the models evolve towards greater realism, and permit sharper comprehension of what factors make a “better” model better.

Acknowledgements

Financial support was provided by the Natural Sciences and Engineering Research Council of Canada (NSERC) and by Environment Canada. I am grateful to Murray Judd and P. Prendergast for permission to cite their pressure data. I also thank Terry Thomson and Cliff Thoreau for their help in setting up the Ellerslie experiment; Terry Nord and Mark Ackerman (Department of Mechanical Engineering) for use of their equipment; and Tom Flesch, Brian Crenna and Curtis Mooney for many profitable discussions of this work.

Appendix A. Magnitude of Topographically-Induced Pressure Field

No field is absolutely level. How may one assess the possible importance of topographic undulations, on these measurements of the pressure field about a windbreak? Jackson and Hunt (1975) gave an analytic theory of windflow over low hills, which may be adapted to the purpose. For a ‘Witch of Agnesi’ ridge, i.e., a ridge with topographic profile

$$Z(x) = \frac{H_z}{1 + (x/H_x)^2} \quad (\text{A1})$$

where H_z is the hill-height and H_x the hill half-length, the maximum pressure perturbation, according to the Jackson-Hunt theory, is

$$\frac{\Delta \bar{p}}{\rho u_{*0}^2} = \frac{1}{k_v^2} \frac{H_z}{H_x} \ln^2 \left(\frac{H_x}{z_0} \right). \quad (\text{A2})$$

Re-scaling on the mean windspeed \bar{u}_{0H} at the height (H) of a windbreak, to permit comparison with the observed pressure variations about a windbreak (Figure 4), this implies

$$\frac{\Delta \bar{p}}{\rho \bar{u}_{0H}^2} = \frac{H_z}{H_x} \frac{\ln^2 \left(\frac{H_x}{z_0} \right)}{\ln^2 \left(\frac{H}{z_0} \right)}. \quad (\text{A3})$$

For the Ellerslie site, with $H = 1.25$ m, $z_0 \approx 0.01$ m, and assuming $H_z/H_x = 1 : 200$, undulations with half-length $H_x \approx 50$ m would have induced normalised pressure variations of order 0.01. Pressure variations induced by the windbreak (see Figure 4) were larger by an order of magnitude.

Appendix B. Time Constant of Tube and Bottle Filter

To determine the effect of the tube-and-bottle filter (Figure 2) upon the measured pressure, consider the pressure drop ($p_0 - p_b$) down a length L_f of the tube, where p_0 is the inlet pressure, and $p_b(t)$ is the ‘responding’ time-damped pressure in the bottle. A dimensionless coefficient of resistance (λ) is conventionally defined by (Schlichting, 1968):

$$\frac{p_0 - p_b}{L_f} = \lambda \frac{\frac{1}{2} \rho U^2}{d} \quad (\text{B1})$$

where d is the tubing diameter, and U is the mean velocity ($U = Q/\pi r^2$, where Q is the volumetric flow rate and $r = d/2$ is the radius). For low Reynolds-number flow ($Re = Ud/\nu < 2300$; ν the kinematic viscosity), as in the present case, $\lambda = 64/Re$.

Now, the ideal gas law applied to the air in the bottle reads

$$p_b(t)V_b = m(t)RT_b \quad (\text{B2})$$

where $R (= 287 \text{ J kg}^{-1} \text{ K}^{-1})$ is the specific gas constant for dry air, and where we will assume that the temperature T_b in the bottle is constant. Differentiating w.r.t. time, and eliminating the mass flow rate dm/dt with the aid of the resistance law, it

is straightforward to determine that the time constant for adjustment of the bottle pressure to a change of the inlet pressure p_0 is:

$$\tau_b = \frac{128 \rho \nu L_f V_b}{\pi p_0 d^4}. \quad (\text{B3})$$

Specifying $L_f = 2$ m, $d = 1/16$ th inch, and $V_b = 4$ litres, the time constant is (theoretically) $\tau_b \approx 9$ sec.

A laboratory determination, by means of observing the step response, gave a larger value, presumably due to the added resistance of the 15 m of larger diameter tubing, and other additional resistances (such as the bottle inlets). An exact figure could not be determined, because of a superposed 'noise' on the step response originating from drifting temperature of the bottle (a factor reduced in the field by burying the bottles). However it is certain that $20 \text{ sec} \leq \tau_b \leq 30 \text{ sec}$. Thus the tube-and-bottle filter averaged out fluctuations in the sample point pressure p_0 on periods less than about 30 sec, implying that a 'return time' of 30 sec between successive samples of each bottle was entirely adequate, and that a much longer return time of 3 min, as used in the final experiments, was probably acceptable.

Appendix C. Pressure Response Correction

The step response of the Setra transducer, whether directly coupled to a calibration pressure-tank or when coupled to that tank through the field configuration (i.e., 1 m of 1/16th ID tubing and through the Scanivalve switch), could be accurately described by the ideal response of a linear, first-order system, i.e., by:

$$p = p_{mx} \left(1 - \exp\left(-\frac{t}{\tau}\right) \right) \quad (\text{C1})$$

where p_{mx} is the pressure-excess in the calibration tank, released at the instant $t = 0$ (p_{mx} was set to the full scale pressure of the transducer). For direct coupling $\tau = \tau_{pt} \approx 0.64$ s, which is essentially the time constant of the transducer itself. However using the 'field coupling', $\tau = \tau_{os} \approx 2$ s.

It had been expected that the (assumed) negligible volume between the outlet of the sample bottle and the Setra would imply that a delay after switching of order $3\tau_{pt}$ (≈ 2 sec) should be quite adequate. In all experiments prior to October 11, 1996, the delay after switching was $t_D = 1.7$ sec. Only after inconsistent pressure fields were obtained on consecutive days, with the sole difference of moving the upstream sample points downstream, was the possibility of a longer effective time constant τ_{os} suspected, and later confirmed in the laboratory.

It was necessary, then, to correct the raw pressure profiles for the slow instrument response. For a continuous linear system such as this, the response $r(t)$ is related to the input signal $s(t)$ as:

$$r(t) = \int_{\xi=0}^{\infty} s(t - \xi) W(\xi) d\xi \quad (\text{C2})$$

where $W(\xi)$ is the ‘system weighting function’, or ‘impulse response function’. Many first-order systems, such as the RC filter, or a thermometer, have

$$W(\xi) = \frac{1}{\tau} \exp\left(-\frac{\xi}{\tau}\right) \tag{C3}$$

where the time constant τ is that manifested in the step response. As expected, and as confirmed by the measured step response, the present system can be treated as a linear first-order system.

In carrying out the response correction on discrete sampled data, it is necessary to assume that the true bottle pressure, here labelled p_c (corrected pressure, playing the role of the signal $s(t)$ in the analysis) was *constant* during the $\Delta t = 2.5$ s over which it was coupled through the Scanivalve to the pressure-transducer (Setra). Because the measured time constant τ_b of the tube and bottle filter was more than 20 sec (see Appendix B), that approximation is quite acceptable. Then if $p_i = p(t_i)$ is the measured pressure at time t_i , sampled at time delay t_D after switching to the i th bottle, we break up the integral in Equation (C2) as

$$p_i = p_{c_i} \int_0^{t_D} W(\xi) d\xi + p_{c_{i-1}} \int_{t_D}^{t_D+\Delta t} W(\xi) d\xi + \dots \tag{C4}$$

where p_{c_i} is the actual (i.e., corrected) pressure in the i th bottle, $p_{c_{i-1}}$ is the corrected pressure in the previous bottle, etc. Then

$$p_i = w_0 p_{c_i} + w_1 p_{c_{i-1}} + w_2 p_{c_{i-2}} + \dots \tag{C5}$$

where since we have a first-order system:

$$w_0 = \int_0^{t_D/\tau} \exp\left(-\frac{\xi}{\tau}\right) d\frac{\xi}{\tau} \tag{C6}$$

$$w_1 = \int_{t_D/\tau}^{t_D/\tau+\Delta t/\tau} \exp\left(-\frac{\xi}{\tau}\right) d\frac{\xi}{\tau} \tag{C7}$$

etc. With $\tau = \tau_{os} = 2$ s, with switching interval $\Delta t = 2.5$ s, and with sampling delay (after switching) $t_D = 1.7$ s, the first five weights are

$$w_0 = 0.573, w_1 = 0.305, w_2 = 0.087, w_3 = 0.025, w_4 = 0.007$$

and sum to 0.997. The implication of these weights is that prior to correction the immediately-downstream pressure sample was ‘contaminated’ by the elevated pressures in the bottles attached to sampling ports immediately upstream from the fence.

There are two alternative and equivalent procedures for carrying out the lag-correction:

C.1. CORRECTION OF THE TWELVE-POINT MEAN PRESSURE PROFILE, ASSUMED PERIODIC

Rather than correct the individual samples, in view of the fact that averaging is a linear operation, it is acceptable to simply correct the time-average pressure profile as follows. The bottle index ranges $1 \leq i \leq 12$: so the twelve measured (but smoothed) pressures p_i in conjunction with the known weights, permit us to determine the original (or 'corrected') pressures p_{ci} . This is a straightforward matrix inversion problem,

$$\underline{P} = \underline{W} \underline{P}_c \rightarrow \underline{P}_c = \underline{W}^{-1} \underline{P} \quad (\text{C8})$$

and in this case with only five non-zero weights, the 'weighting matrix' is:

$$\underline{W} = \begin{pmatrix} w_0 & 0 & 0 & 0 & 0 & 0 & 0 & 0 & 0 & w_4 & w_3 & w_2 & w_1 \\ w_1 & w_2 & 0 & 0 & 0 & 0 & 0 & 0 & 0 & 0 & w_4 & w_3 & w_2 \\ w_2 & w_1 & w_0 & 0 & 0 & 0 & 0 & 0 & 0 & 0 & 0 & w_4 & w_3 \\ w_3 & w_2 & w_1 & w_0 & 0 & 0 & 0 & 0 & 0 & 0 & 0 & 0 & w_4 \\ w_4 & w_3 & w_2 & w_1 & w_0 & 0 & 0 & 0 & 0 & 0 & 0 & 0 & 0 \\ 0 & w_4 & w_3 & w_2 & w_1 & w_0 & 0 & 0 & 0 & 0 & 0 & 0 & 0 \\ 0 & 0 & w_4 & w_3 & w_2 & w_1 & w_0 & 0 & 0 & 0 & 0 & 0 & 0 \\ 0 & 0 & 0 & w_4 & w_3 & w_2 & w_1 & w_0 & 0 & 0 & 0 & 0 & 0 \\ 0 & 0 & 0 & 0 & w_4 & w_3 & w_2 & w_1 & w_0 & 0 & 0 & 0 & 0 \\ 0 & 0 & 0 & 0 & 0 & w_4 & w_3 & w_2 & w_1 & w_0 & 0 & 0 & 0 \\ 0 & 0 & 0 & 0 & 0 & 0 & w_4 & w_3 & w_2 & w_1 & w_0 & 0 & 0 \\ 0 & 0 & 0 & 0 & 0 & 0 & 0 & w_4 & w_3 & w_2 & w_1 & w_0 & 0 \\ 0 & 0 & 0 & 0 & 0 & 0 & 0 & 0 & w_4 & w_3 & w_2 & w_1 & w_0 \end{pmatrix}. \quad (\text{C9})$$

Matrix inversion algorithms may be found in Press et al. (1988).

C.2. LAG-CORRECTION OF THE ENTIRE DATA SEQUENCE

It is also possible to rearrange Equation (C5) as

$$p_{ci} = \frac{1}{w_0} p_i - \frac{w_1}{w_0} p_{c_{i-1}} - \frac{w_2}{w_0} p_{c_{i-2}} + \dots \quad (\text{C10})$$

Except for the first few (4, in this case) members of the data sequence, this equation can be used to perform a sequential lag-correction of the entire 'raw' sequence of pressure-data. That corrected series is then partitioned (by bottle), and averaged. As one expects, this alternative method gives a corrected mean pressure field almost identical to that obtained by method A. The small differences (at the third or fourth significant figure) are due to the necessity of neglecting the lag-correction of the first few members of the data sequence.

Figure C1 gives the raw mean pressure profile, and the corrected profile, for the period 1301–1330 on October 7, 1996 (also shown are the lag-corrected 'zeroes').

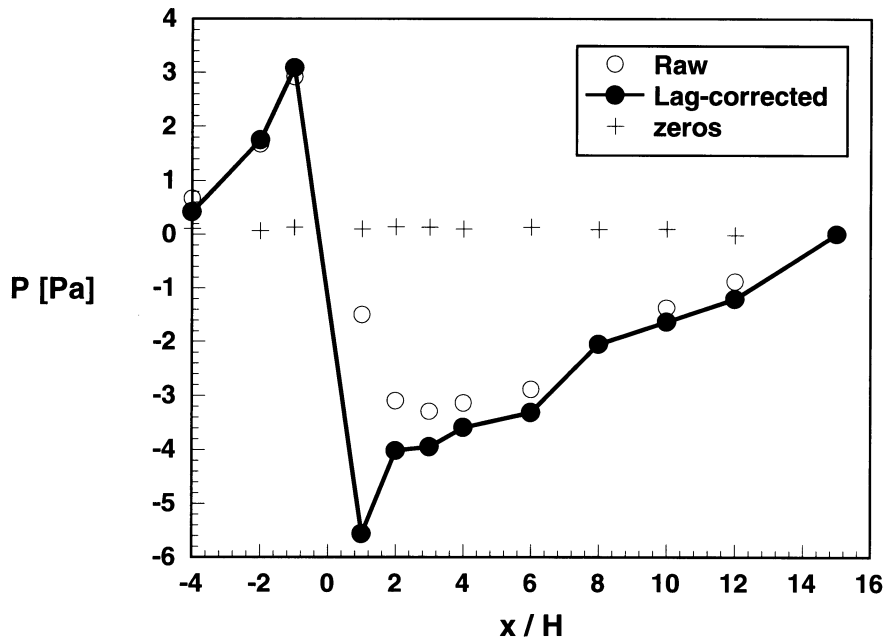


Figure C1. 'Raw' and 'lag-corrected' mean pressure profile [Pa] for the period 1301–1330, 7 October, 1996, during which interval $u_{*0} = 0.46 \text{ m s}^{-1}$ and $\bar{u}_{0H} \sim 6 \text{ m s}^{-1}$. Also shown are the (lag-corrected) 'zeros' measured on the interval 1620–1644 on the same day. Unfortunately the 'zeros' were not checked earlier in the day – for this profile (and others collected on October 7) reveals a pressure plateau of sorts in the leeward region.

Clearly the correction is absolutely critical, since the shape of the pressure profile is the subject of this paper. Note that the original (measured) pressure profile is 'smoother' than the proper, lag-corrected profile, – this should be no surprise, since the error to be corrected was a smoothing error (measurement influenced by earlier data). The fact that data collected with sampling interval $\Delta t = 15 \text{ sec}$ are similar to the comparable lag-corrected $\Delta t = 2.5 \text{ sec}$ data (see Figure 4) is additional evidence of the validity of the lag-correction.

References

- Argete, J. C. and Wilson, J. D.: 1989, 'The Microclimate in the Centre of Small Square Sheltered Plots', *Agric. For. Meteorol.* **48**, 185–199.
- Bradley, E. F. and Mulhearn, P. J.: 1983, 'Development of Velocity and Shear Stress Distributions in the Wake of a Porous Shelter Fence', *J. Wind Eng. Indust. Aerodyn.* **15**, 145–156.
- Cowan, I. R.: 1968, 'Mass, Heat and Momentum Exchange Between Stands of Plants and Their Atmospheric Environment', *Quart. J. Roy. Meteorol. Soc.* **94**, 523–544.
- Finnigan, J. J. and Bradley, E. F.: 1983, 'The Turbulent Kinetic Energy Budget Behind a Porous Barrier: An Analysis in Streamline Coordinates', *J. Wind Eng. Indust. Aerodyn.* **15**, 157–168.
- Hagen, L. J., Skidmore, E. L., Miller, P. L., and Kipp, J. E.: 1981, 'Simulation of Effect of Wind Barriers on Windflow', *Trans. ASAE* **24**, 1002–1008.

- Jacobs, A. F. G.: 1984, 'Static Pressure Around a Thin Barrier', *Arch. Met. Biocl., Ser. B* **35**, 127–135.
- Jackson, P. S. and Hunt, J. C. R.: 1975, 'Turbulent Wind Flow Over a Low Hill', *Quart. J. Roy. Meteorol. Soc.* **101**, 929–955.
- Judd, M. J., Raupach, M. R., and Finnigan, J. J.: 1996, 'A Wind Tunnel Study of Turbulent Flow Around Single and Multiple Windbreaks, Part I: Velocity Fields', *Boundary-Layer Meteorol.* **80**, 127–165.
- Judd, M. J. and Prendergast, P. T.: 1996, 'Pressure and Turbulence Measurements Around a Windbreak', Internal Report No. 96/220, Hort. & Food Res. Inst. P.O. Box 23, Kerikeri, New Zealand.
- Launder, B. E., Reece, G. J., and Rodi, W.: 1975, 'Progress in the Development of a Reynolds-Stress Turbulence Closure', *J. Fluid Mech.* **68**, 537–566.
- Patankar, S. V.: 1980, *Numerical Heat Transfer and Fluid Flow*, Series in Computational Methods in Mechanics and Thermal Sciences, Hemisphere Publishing Co., London, 197 pp.
- Patankar, S. V.: 1981, 'A Calculation Procedure for Two-Dimensional Elliptic Situations', *Numerical Heat Transfer* **4**, 409–425.
- Patton, E. G., Sullivan, P. P., Shaw, R. H., Paw U, K. T., and Moeng, C. H.: 1996, 'A Nested-Grid Large Eddy Simulation of Turbulent Flow Above and Within a Forest', Preprint volume for 22nd Conference of the AMS on Agric. Forest Meteorol., Atlanta, pp. J41–J42.
- Press, W. H., Flannery, B. P., Teukolsky, S. A., and Vetterling, W. T.: 1988, *Numerical Recipes in C*, Cambridge University Press, Cambridge, 735 pp.
- Schlichting, H.: 1968, *Boundary-Layer Theory*, 6th edition, McGraw-Hill, 748 pp.
- Schmidt, R. A., Takle, E. S., Brandle, J. R., and Litvina, I. V.: 1995, 'Static Pressure at the Ground Under Atmospheric Flow Across a Windbreak', Preprint volume for 11th Symposium of the AMS on Boundary Layers and Turbulence, Charlotte, NC, pp. 517–520.
- Schwartz, R. C., Fryrear, E. W., Harris, B. L., Bilbro, J. D., and Juo, A. S. R.: 1995, 'Mean Flow and Shear Stress Distributions as Influenced by Vegetative Windbreak Structure', *Agric. For. Meteorol.* **75**, 1–22.
- Takle, E. S. and Wang, H.: 1997, 'Reply to Comments by J. D. Wilson and C. J. Mooney', *Boundary-Layer Meteorol.* **85**, 151–159.
- Wang, H. and Takle, E. S.: 1995, 'A Numerical Simulation of Boundary-Layer Flows Near Shelterbelts', *Boundary-Layer Meteorol.* **75**, 141–173.
- Wang, H. and Takle, E. S.: 1996a, 'On Three-Dimensionality of Shelterbelt Structure and Its Influences on Shelter Effects', *Boundary-Layer Meteorol.* **79**, 83–105.
- Wang, H. and Takle, E. S.: 1996b, 'Momentum Budget and Shelter Mechanism of Boundary-Layer Flow Near a Shelterbelt', *Boundary-Layer Meteorol.* **82**, 417–435.
- Wilson, J. D. and Mooney, C. J.: 1997, 'Comments on "A Numerical Simulation of Boundary-Layer Flows Near Shelterbelts" by H. Wang and E. Takle', *Boundary-Layer Meteorol.* **85**, 137–149.
- Wilson, J. D., Finnigan, J. J., and Raupach, M. R.: 1997, 'A First-Order Closure for Disturbed Plant Canopy Flows, and Its Application to Windflow Through a Canopy on a Ridge', *Quart. J. Roy. Meteorol. Soc.*, in press.
- Wilson, J. D., Swaters, G. E., and Ustina, F.: 1990, 'A Perturbation Analysis of Turbulent Flow Through a Porous Barrier', *Quart. J. Roy. Meteorol. Soc.* **116**, 989–1004.
- Wilson, J. D.: 1988, 'A Second-Order Closure Model for Flow Through Vegetation', *Boundary-Layer Meteorol.* **42**, 371–392.
- Wilson, J. D.: 1985, 'Numerical Studies of Flow Through a Windbreak', *J. Wind Eng. Indust. Aerodyn.* **21**, 119–154.
- Wilson, N. R. and Shaw, R. H.: 1977, 'A Higher Order Closure Model for Canopy Flow', *J. Appl. Meteorol.* **16**, 1197–1205.